Mini Review

Cytochrome *c*: Surfing Off of the Mitochondrial Membrane on the Tops of Complexes III and IV

Gonzalo Pérez-Mejías [1], Alejandra Guerra-Castellano [1], Antonio Díaz-Quintana, Miguel A. De la Rosa, Irene Díaz-Moreno *

Instituto de Investigaciones Químicas (IIQ), Centro de Investigaciones Científicas Isla de la Cartuja (cicCartuja), Universidad de Sevilla – Consejo Superior de Investigaciones Científicas (CSIC), Avda. Américo Vespucio 49, Sevilla 41092, Spain

A B S T R A C T

The proper arrangement of protein components within the respiratory electron transport chain is nowadays a matter of intense debate, since altering it leads to cell aging and other related pathologies. Here, we discuss three current views—the so-called *solid*, *fluid* and *plasticity* models—which describe the organization of the main membrane-embedded mitochondrial protein complexes and the key elements that regulate and/or facilitate supercomplex assembly. The soluble electron carrier cytochrome *c* has recently emerged as an essential factor in the assembly and function of respiratory supercomplexes. In fact, a 'restricted diffusion pathway' mechanism for electron transfer between complexes III and IV has been proposed based on the secondary, *distal* binding sites for cytochrome *c* at its two membrane partners recently discovered. This channeling pathway facilitates the surfing of cytochrome *c* on both respiratory complexes, thereby tuning the efficiency of oxidative phosphorylation and diminishing the production of reactive oxygen species. The well-documented post-translational modifications of cytochrome *c* could further contribute to the rapid adjustment of electron flow in response to changing cellular conditions.

Contents

1. Introduction

Mitochondria are the powerhouses of the cell, generating the greatest amount of chemical energy in the form of ATP during cellular respiration. During respiration electrons from reduced nicotinamide adenine dinucleotide (NADH) and reduced flavin adenine dinucleotide ($FADH_2$) are transferred via the electron transport chain (ETC) to molecular oxygen (O_2). Electron flow through the ETC is coupled with the generation of an electrochemical proton gradient across the inner mitochondrial membrane that in turn yields ATP, a process known as oxidative phosphorylation (OxPhos) [1].

The ETC has four transmembrane protein complexes: complex I (CI; NADH-ubiquinone oxidoreductase), complex II (CII; succinate-ubiquinone reductase), complex III (CIII; cytochrome bc_1 complex) and complex IV (CIV; cytochrome *c* oxidase). In addition to the transmembrane complexes, two mobile carriers participate in the OxPhos

process: lipophilic ubiquinone (Q) and hydrophilic cytochrome *c* (C*c*), which transfer electrons from CI/CII to CIII and from CIII to CIV, respectively. The electrochemical proton gradient generated by the ETC complexes (except CII which does not pump H$^+$) drives the synthesis of ATP through complex V (CV; ATP synthase). Beyond the ETC components abovementioned, several mitochondrial enzymes—namely, electron-transferring flavoprotein Q oxidoreductase, dihydroorotate dehydrogenase or glycerol-3-phosphate dehydrogenase—may act as auxiliary elements of the respiratory chain [2].

The organization and dynamics of protein components within the ETC is currently a matter of debate. Three different models have been proposed to explain their organization (Fig. 1). On one hand, the *fluid* model states that the membrane components diffuse freely and independently [3] (Fig. 1A, *right* panel). While on the other hand, the *solid* model proposes that respiratory complexes are stably associated forming supercomplexes, thus facilitating the flow of electrons [4,5] (Fig. 1A, *left* panel). However, the idea that these two scenarios are not exclusive gave rise to the *plasticity* model; this model consists of a balanced distribution between free respiratory complexes and supercomplexes, adapting the efficiency of the ETC by means of partitioned Q and C*c* pools [6] (Fig. 1B).

Supercomplex formation occurs in mammals, plants, yeast and some bacteria [7–9]. Among these supercomplexes, one stands out; the respirasome, which contains CI, CIII and CIV and is capable of NADH: O$_2$ oxidoreduction *in vitro* [10]. The degree of association and the
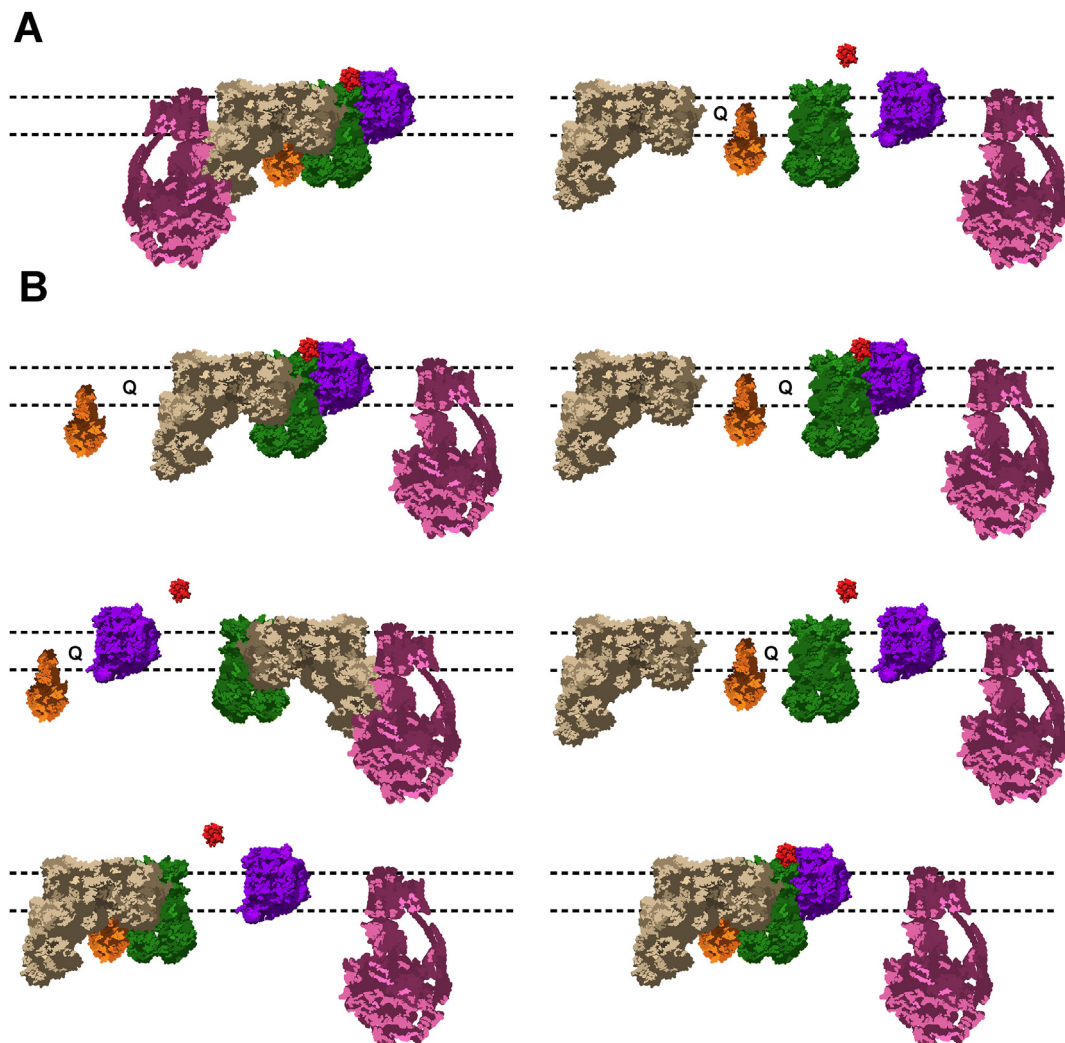
stoichiometries of respiratory complexes in supercomplexes depend on cell type, tissue-specific isoforms and cellular conditions [11–14]. The mitochondrial intermembrane lipid content also affects supercomplex assembly [15–18].

The diverse composition and stoichiometry of supercomplexes has been evidenced by blue native polyacrylamide gel electrophoresis (BN-PAGE), cryo-electron tomography and single-particle electron microscopy studies of mitochondrial fractions solubilized with mild detergents. Fig. 1B represents the different supercomplexes described in the literature. In brief, CI mainly interacts with CIII and CIV to form the respirasome (CI + CIII$_2$ + CIV$_{1–4}$) [10,19–26]. Alternatively, CIII binds to CI (CI + CIII$_2$) or CIV as a monomer (CIII$_2$ + CIV$_{1–2}$) [7,22,23,25,27,28]. Generally speaking, CV assembles oligomers and CII acts as a stand-alone complex. However, their associations with complexes I, III, and IV have also been described [25,27].

2. Key Elements for Respiratory Supercomplex Assembly

The mechanisms which regulate the assembly of mitochondrial supercomplexes remain unsolved. However, several biomolecules have been recently described to regulate/facilitate the formation of certain supercomplexes.

As mentioned above, phospholipids mediate protein-protein interactions within the inner mitochondrial membrane. Cardiolipin—an anionic phospholipid found primarily in the inner mitochondrial

Fig. 1. Schematic representation of the organization of respiratory complexes. A) *Solid* (*left*) and *fluid* (*right*) models. B) *Plasticity* model. All supercomplexes described in the literature are displayed. The stoichiometry of each respiratory complex is not represented. CI is in tan, CII in orange, CIII in green, CIV in purple, CV in pink, C*c* in red and ubiquinone as Q.

membrane—represents 20% of all membrane lipids [29]. Lack of cardiolipin has been linked with metabolic disorders, such as Barth's Syndrome, and affects the stability of supercomplexes and the activity of CIV [30]. Phosphatidylethanolamine is a cationic phospholipid present in all cellular membranes which when depleted favours the formation of large supercomplexes [17]. Therefore, the distribution of phospholipids may play an important role in the reorganization of respiratory complexes into supercomplexes.

Several proteins have been postulated to function as chaperones or assembly factors for supercomplexes. For instance, the depletion of 28 different NADH:ubiquinone oxidoreductase supernumerary subunits (NDUF) out of 30, which are necessary for CI assembly and stability, has also been described to reduce supercomplexes containing CI + CIII$_2$ and CI + CIII$_2$ + CIV$_1$ in human cells [31]. Although the transmembrane NDUFA4 subunit has initially been defined as a component of CI, new reports suggest that it belongs to CIV [32,33]. Interestingly enough, NDUFA4 has recently been postulated as a factor required for assembly of supercomplexes in growing cells and cancer tissues [34]. The MJC/DnaJC15 protein, a mitochondrial repressor of the ETC that interacts with CI, has been described as a regulator of supercomplex formation [35].

Recently, the CIV subunit COX7A2L (also known as SCAFI) has been proposed as a CIII binding protein which stabilizes the CIII$_2$ + CIV$_1$ supercomplex, independently of respirasome formation [36,37]. In yeast, two respiratory complex factors (Rcf1 and Rcf2), members of the conserved hypoxia induced gene 1 (Hig1) protein family, regulate the formation and stabilization of the CIII$_2$ + CIV$_{1-2}$ supercomplex [38–40]. Rcf1 has two eukaryotic orthologues, namely HIG1 hypoxia inducible domain family 1A and 2A (HIGD1A and HIGD2A, respectively). Indeed, HIGD2A knockdown causes depletion of the CIII$_2$ + CIV$_1$ supercomplex [41]. Further, the ADP/ATP carrier protein has been reported to exist in association with CIII$_2$ + CIV$_2$ and mediates such supercomplex assembly in yeast [42]. Prohibitin has been hypothesized to act as a chaperone in aiding the assembly of respiratory complexes—in particular CI [43]. Indeed, recent data indicates that the CIII$_2$ + CIV supercomplex content decreases in the absence of prohibitin [44].

Finally, the ETC mobile carriers Q and Cc co-migrate with supercomplexes in BN-PAGE analyses [27]. Strikingly, the absence of Cc destabilizes CI and CIV [45].

3. Cytochrome *c*: An Efficient Electron Carrier between CIII and CIV

Cc is an essential metalloprotein for mitochondrial metabolism and homeostasis, playing a dual-purpose role in cell life and death [46–48]. Under homeostasis, Cc acts as electron carrier within the respiratory chain in the mitochondria. Voltammetry assays and current crystal structures of CIII and CIV complexed with Cc resolve only one Cc molecule per monomer [49–51]. However, earlier reports had suggested the existence of additional binding sites in both CIII and CIV [52–56]. Multiphasic kinetics observed in early assays for the oxidation of reduced Cc by CIV can be fitted to a model with just one catalytic site. Such a simple model includes alternative binding conformations of the transient complex, with some of them being unable to transfer electrons but affecting the ET rate at the catalytic site [53,57]. Direct Cc-CcO binding studies performed by gel filtration evidenced a 2:1 stoichiometry, in which Cc bound at a first site with a low dissociation constant and at a second site with less affinity [49]. Non-ET conformations within the complex between CIII and Cc were also evidenced by steady state kinetic analysis, and so a binding model with more than one molecule of Cc per molecule of CIII was proposed to explain the observed multiphasic kinetics [58]. More recently, *in solution* nuclear magnetic resonance (NMR) and isothermal titration calorimetry (ITC) experiments have confirmed the presence of a secondary binding site on cytochrome c_1 (Cc_1) for Cc, with an affinity 10-fold lower than that of the principal binding site [59,60]. The two Cc-binding sites of Cc_1 in CIII were named *proximal* and *distal*, according to Brownian Dynamics (BD) calculations and NMR-driven docking computations (Fig. 2). In the *proximal* site, the heme groups of Cc and Cc_1 lay near each other, allowing electron transfer. The interaction surface on Cc involves a hydrophobic patch around the heme cleft surrounded by positively charged residues. Such binding surface configuration determines the correct orientation of Cc towards the heme group of Cc_1 and is common to other ET complexes [61,62]. However, the surface used by Cc to bind the *distal* site of Cc_1 is less-well defined when compared with the *proximal* one, in agreement with its lower affinity. Furthermore, the *distal* site lies far from the heme pocket of Cc_1, meaning there is low compatibly at the secondary site for efficient electron transfer.

Secondary binding sites may play multiple roles in ETCs, including photosynthetic ones. For instance, in eukaryotic Photosystem I [63], secondary binding sites assure fast replacement of electron donor
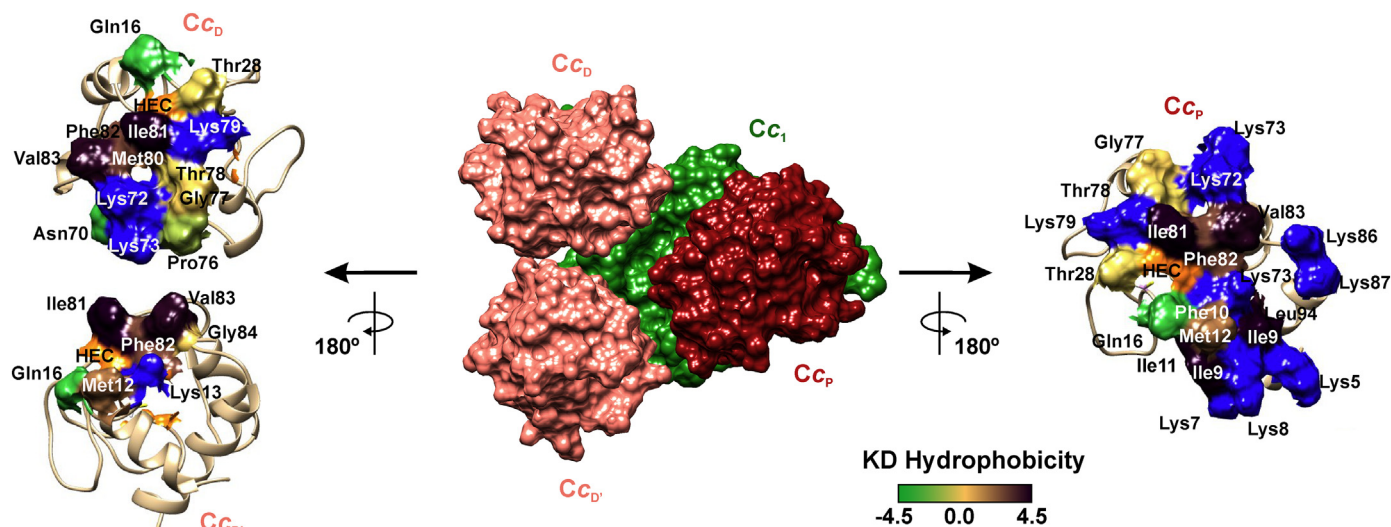
Fig. 2. Binding surfaces of cytochrome *c* on cytochrome c_1. Brownian Dynamics calculations and NMR-driven docking computations accommodate three Cc molecules in the soluble domain of cytochrome c_1. In the middle panel, two Cc molecules are located at the *distal* sites of cytochrome c_1 (Cc_D and C$c_{D'}$), whereas one Cc molecule is at the *proximal* site of cytochrome c_1 (Cc_P). On *left* and *right* panels, Cc molecules are rotated 180° to expose interaction areas, with the residues colored according to the Kyte and Doolittle (KD) hydrophobicity scale; basic residues are in blue and the heme group (HEC) is in orange. Pictures were created with the UCFS Chimera software using the PDB structures for CIV (5XTH) and Cc (2N9I) [88].
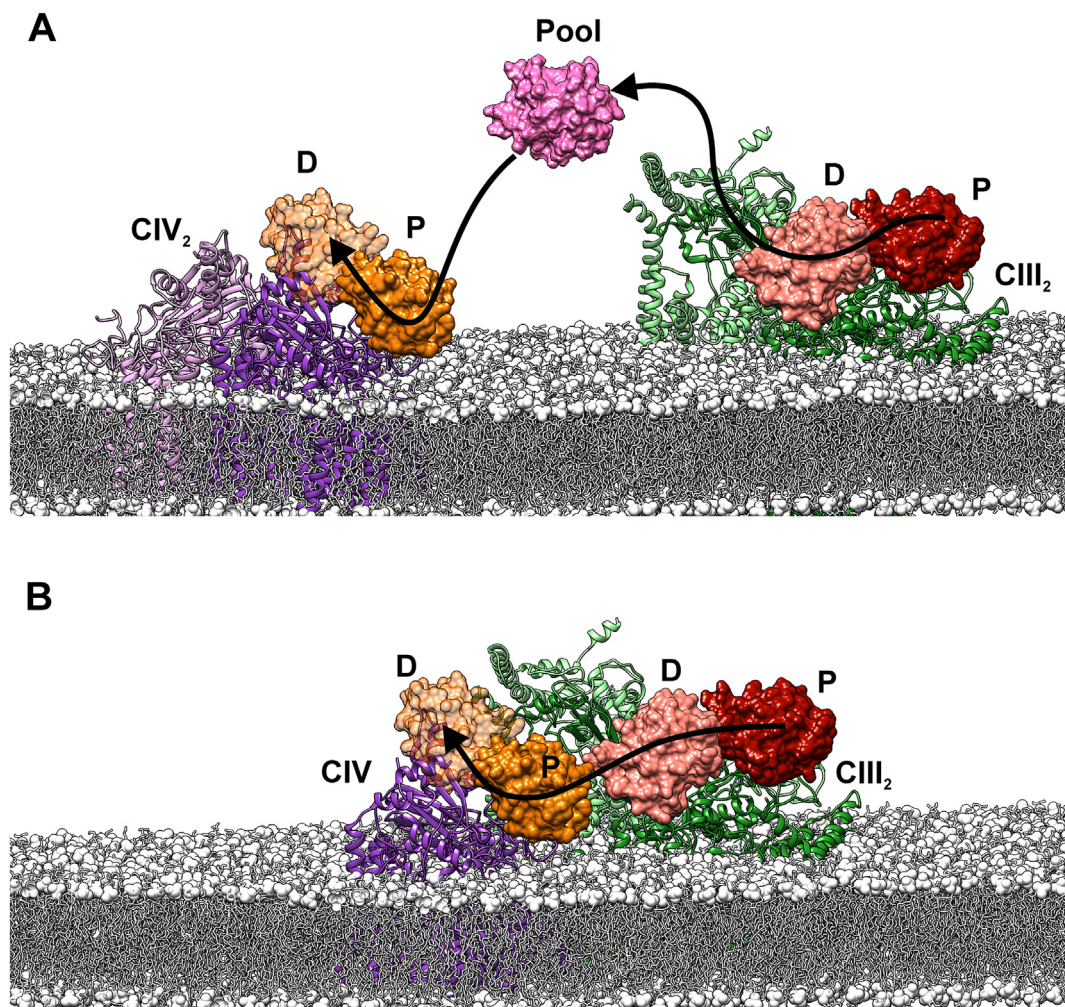
Fig. 3. Cytochrome *c* molecules surfing between respiratory complexes. A) *Fluid* model of dimeric CIII (green) and dimeric CIV (purple) embedded in the mitochondrial membrane. Isolated CIV is classically a dimer, as inferred from X-ray crystal structures [87]. B) *Solid* model of dimeric CIII and monomeric CIV, as shown in the recent Cryo-EM structure for human respiratory supercomplex complex [26]. P and D respectively stand for *distal* and *proximal* C*c* binding sites on each complex. "Pool" denotes C*c* population within the bulk intermembrane space. Pictures were created with the UCFS Chimera software using the PDB structures for CIII, CIV (5XTH) and cytochrome *c* (2N9I) [88].

molecules once an ET reaction takes place, and disabling them is lethal. In the context of supercomplexes, these additional *distal* sites at CIII and CIV could facilitate the channeling of electron carriers by building a 're-stricted diffusion pathway' for C*c* molecules across the surface of the two mitochondrial respiratory complexes instead of carrying electrons by random diffusion across de intermembrane mitochondrial space (Fig. 3). This fractal diffusion pathway substantially increases the efficiency of the OxPhos process in respect to the bulk 3D search, and decreases the production of reactive oxygen species (ROS) [64,65]. Indeed, restraining diffusion by weak interactions with membranes, cytoskeletal structures and DNA substantially lowers the time a molecule needs to reach its target [66]. Both effects—increasing turnover and restraining diffusion of mobile carriers between two membrane complexes—are clear advantages of secondary sites in ETCs.

4. Functional Implications of Post-Translational Modifications of Cytochrome *c*

The ETC is tightly regulated by post-translational modifications (PTMs), widening the function of its components under homeostatic and stress conditions [67,68]. Notably, the structure and activity of C*c* are controlled *in vivo* by phosphorylation of threonine 28, serine 47 and tyrosine 48 and 97 [69–79].

Because of the low yield of most phosphorylated C*c* species obtained from cell extracts and the specific C*c* kinase being unknown, phosphomimic C*c* variants are the best alternative approach to analyze the effect of C*c* phosphorylation [76,80,81]. Actually, an extensive study of the functional effect of phosphorylation is unfeasible with purified phosphorylated C*c* species, but can be performed in an equivalent way with phosphomimic mutants.

Traditionally, tyrosine phosphorylation has been mimicked by mutating tyrosine to glutamate/aspartate. However, it has recently been established that the substitution of tyrosine with the non-canonical amino acid *p*-carboxymethyl-L-phenylalanine (*p*CMF) better mirrors tyrosine phosphorylation. Notably, all mutants maintain the 2:1 stoichiometry (C*c*:C*c*$_1$ and C*c*:CIV) found for the wild-type (WT) species. Nevertheless, whereas all tested phosphomimetic C*c* species show similar affinities for the *proximal site* at C*c*$_1$ (Table 1), binding at the *distal site* is substantially hindered by the additional negative charge of C*c* [75,77]. The affinity of C*c* towards bovine CIV changes depending on the residue of C*c* that is phosphorylated (Table 1) [65,77].

As noted in the Introduction section, the formation of supercomplexes has been proposed to increase ET efficiency during OxPhos, thereby minimizing the generation of ROS. ROS are generally generated in complexes I and III, and can damage key components of cells [82,83]. The OxPhos process has been determined by the ability

Table 1
Effect of post-translational modifications on cytochrome c binding and activity assays.

Cc species	Affinity towards CIII[a]		Affinity towards CIV		CcO activity		
	Proximal site	Distal site	Proximal site	Distal site	Fluid[b]	Fluid[c]	Solid[d]
T28D [75]	~	↓	n.d.	n.d.	↑		n.d.
T28E [76]	n.d.	n.d.	n.d.	n.d.		↓↓	
pT28 [76]	n.d.	n.d.	n.d.	n.d.		↓↓	n.d.
S47D [75]	~	~	n.d.	n.d.	↑		n.d.
Y48pCMF [77]	~	↓	↓	↓↓↓	↑		↓
pY48 [78]	n.d.	n.d.	n.d.	n.d.		↓	n.d.
Y97pCMF [65]	n.d.	n.d.	↑↑↑	↑↑↑	↑		↑↑
pY97 [70]	n.d.	n.d.	n.d.	n.d.		↓↓	n.d.

n.d.: not determined.

'Fluid' and 'Solid' refer to the two proposed models in which ETC are organised in the inner mitochondrial membrane.

  [a] Affinity determined with the soluble N-terminal domain of *Arabidopsis thaliana* cytochrome c_1.

  [b] Activity measured as Cc oxidation by CIV isolated from bovine or equine heart.

  [c] Activity measured as O_2 consumption by CIV isolated from bovine tissues under conditions preserving the enzyme phosphorylation status.

  [d] Activity measured as Cc oxidation in isolated yeast mitochondria.

of Cc to shuttle electrons to CIV. When Cc performs a three-dimensional search visiting the bulk of the intermembrane mitochondrial space, every well-described phosphorylation in Cc enhances the cytochrome c oxidase (CcO) activity *in vitro*, in Cc oxidation assays using commercial CIV from bovine or equine heart (Table 1) [65,75,77]. Nevertheless, CIV isolated from bovine tissues under conditions preserving the phosphorylation status of CcO shows increased K_M values for phosphorylated Cc species and T28E mutant in O_2 consumption assays [70,76,78]. Thus, simultaneous phosphorylation of both heme-containing proteins, Cc and CcO, could act synergistically in inhibiting CcO activity. This apparent discrepancy could mainly be ascribed to PTMs of CcO.

When CcO activity is measured in mitochondria from cells grown in medium promoting the CIII-CIV supercomplex assembly (as part of the *solid* model), the Y48pCMF mutation decreases the electron donor ability of Cc towards CcO. In contrast, *in vitro* observations mimicking the *fluid* model enhance Cc oxidation (Table 1). In the context of the *fluid* model, the *proximal sites* for Cc on CIII and CIV govern ET reactions. However, in the *solid* model, the *distal sites*, which are non-ET functional sites, become important in limiting the diffusion of Cc molecules on the respiratory CIII-CIV supercomplex.

The balance between relative affinities towards the *proximal* and *distal* sites of CIII and CIV determines Cc exchange rates, alike in photosynthetic membrane complexes [63]. Indeed, the higher affinity of reduced Y48pCMF Cc towards the *proximal* site at CIII impairs its replacement by a new, oxidized Cc molecule. Further, the channeling of Cc molecules at the CIII-CIV ensemble would be disrupted by its weaker binding to the *distal* sites, altogether affecting steady-state, CcO-dependent oxidation rate of Cc (Table 1) [77]. On the other hand, in the assays with isolated CIV, a decrease in the binding affinities may inhibit CcO activity [78], although an increased turnover could yield the opposite under steady-state conditions [77] (Table 1).

In addition, the higher affinity of Y97pCMF Cc towards both the *proximal* and *distal* sites of CIV could facilitate the electron Cc-CcO flow and the pathway of Cc molecules on CIII-CIV supercomplexes [65]. Although Tyr97 in WT Cc is far from the adduct interface [51,84], its phosphorylation may affect long-range interactions, Cc dynamics and/or its orientation within the complex.

To sum up, phosphorylation of Cc regulates the physico-chemical properties—such as alkaline transition, redox potential, stability, affinity towards partners, among others—that are essential for shuttling electrons. This would enable the rapid adjustment of Cc function to changing cellular conditions.

5. Concluding Remarks

According to the data herein reviewed, Cc plays a major regulatory role in OxPhos owing to its highly dynamic interactions with redox targets, and displays a fast turnover during the electron exchange cycle. Multiple binding sites in Cc partners are essential to facilitate Cc turnover and to define the diffusion pathway of the electron carrier. The effectiveness of such a constraint relies on the ability of cells to modulate both the intricate arrangements of ETC complexes into higher-order assemblies and the ample set of PTMs on Cc and other ETC components. Whereas PTMs of CI, CIII and CIV could regulate their organization into supercomplexes, PTMs of Cc could control the binding mode and affinity between the hemeprotein and its partners (CIII and CIV). In this context, the 'restricted diffusion pathway' of Cc molecules between CIII and CIV could generate a large encounter ensemble of Cc on the surface of ETC complexes previously assembled in supercomplexes, in which the hemeprotein would adopt several orientations in equilibrium with stereospecific positioning. In addition, the extra regulation layer of OxPhos activity by post-translational phosphorylation of Cc could be essential to control oxygen consumption and the generation of harmful reactive species during homeostasis and pathology. Cc—either phosphorylated or not—might play additional roles in aiding the assembly of ETC membrane complexes or even supercomplexes. Actually, the lack of Cc disrupts the stability/assembly of CIV in yeasts, mammals and plants [45,85,86] and the hemeprotein migrates with CIII and CIV in BN-PAGE assays [27].

Conflict of Interests

All authors declare no conflict of interest.

References

[1] Reid RA, Moyle J, Mitchell P. Synthesis of adenosine triphosphate by a proton-motive force in rat liver mitochondria. Nature 1966;212:257–8.

[2] Lenaz G, Genova ML. Structure and organization of mitochondrial respiratory complexes: a new understanding of an old subject. Antioxid Redox Signal 2010;12: 961–1008.

[3] Hackenbrock CR, Chazotte B, Gupte SS. The random collision model and a critical assessment of diffusion and collision in mitochondrial electron transport. J Bioenerg Biomembr 1986;18:331–68.

[4] Chance B, Williams GR. A method for the localization of sites for oxidative phosphorylation. Nature 1955;176:250–4.

[5] Lapuente-Brun E, Moreno-Loshuertos R, Acín-Pérez R, Latorre-Pellicer A, Colás C, Balsa E, et al. Supercomplex assembly determines electron flux in the mitochondrial electron transport chain. Science 2013;340:1567–70.

[6] Acín-Pérez R, Enriquez JA. The function of the respiratory supercomplexes: the plasticity model. Biochim Biophys Acta 2014;1837:444–50.

[7] Schägger H, Pfeiffer K. Supercomplexes in the respiratory chains of yeast and mammalian mitochondria. EMBO J 2000;19:1777–83.

[8] Eubel H, Heinemeyer J, Braun HP. Identification and characterization of respirasomes in potato mitochondria. Plant Physiol 2004;134:1450–9.

[9] Stroh A, Anderka O, Pfeiffer K, Yagi T, Finel M, Ludwig B, et al. Assembly of respiratory complexes I, III, and IV into NADH oxidase supercomplex stabilizes complex I in *Paracoccus denitrificans*. J Biol Chem 2004;279:5000–7.

[10] Schäfer E, Seelert H, Reifschneider NH, Krause F, Dencher NA, Vonck J. Architecture of active mammalian respiratory chain supercomplexes. J Biol Chem 2006;281: 15370–5.

[11] Fukuda R, Zhang H, Kim JW, Shimoda L, Dang CV, Semenza GL. HIF-1 regulates cytochrome oxidase subunits to optimize efficiency of respiration in hypoxic cells. Cell 2007;129:111–22.

[12] Ikeda K, Shiba S, Horie-Inoue K, Shimokata K, Inoue S. A stabilizing factor for mitochondrial respiratory supercomplex assembly regulates energy metabolism in muscle. Nat Commun 2013;4:2147.

[13] Genova ML, Lenaz G. Functional role of mitochondrial respiratory supercomplexes. Biochim Biophys Acta 2014;1837:427–43.

[14] Sun D, Li B, Qiu R, Fang H, Lyu J. Cell type-specific modulation of respiratory chain supercomplex organization. Int J Mol Sci 2016;17.

[15] Zhang M, Mileykovskaya E, Dowhan W. Gluing the respiratory chain together. Cardiolipin is required for supercomplex formation in the inner mitochondrial membrane. J Biol Chem 2002;277:43553–6.

[16] Pfeiffer K, Gohil V, Stuart RA, Hunte C, Brandt U, Greenberg ML, et al. Cardiolipin stabilizes respiratory chain supercomplexes. J Biol Chem 2003;278:52873–80.

[17] Böttinger L, Horvath SE, Kleinschroth T, Hunte C, Daum G, Pfanner N, et al. Phosphatidylethanolamine and cardiolipin differentially affect the stability of mitochondrial respiratory chain supercomplexes. J Mol Biol 2012;423:677–86.

[18] Tasseva G, Bai HD, Davidescu M, Haromy A, Michelakis E, Vance JE. Phosphatidylethanolamine deficiency in mammalian mitochondria impairs oxidative phosphorylation and alters mitochondrial morphology. J Biol Chem 2013;288:4158–73.

[19] Schäfer E, Dencher NA, Vonck J, Parcej DN. Three-dimensional structure of the respiratory chain supercomplex $I_1III_2IV_1$ from bovine heart mitochondria. Biochemistry 2007;46:12579–85.

[20] Dudkina NV, Kudryashev M, Stahlberg H, Boekema EJ. Interaction of complexes I, III, and IV within the bovine respirasome by single particle cryoelectron tomography. Proc Natl Acad Sci U S A 2011;108:15196–200.

[21] Althoff T, Mills DJ, Popot JL, Kühlbrandt W. Arrangement of electron transport chain components in bovine mitochondrial supercomplex $I_1III_2IV_1$. EMBO J 2011;30: 4652–64.

[22] Letts JA, Fiedorczuk K, Sazanov LA. The architecture of respiratory supercomplexes. Nature 2016;537:644–8.

[23] Sousa JS, Mills DJ, Vonck J, Kühlbrandt W. Functional asymmetry and electron flow in the bovine respirasome. Elife 2016;5:e21290.

[24] Wu M, Gu J, Guo R, Huang Y, Yang M. Structure of mammalian respiratory supercomplex I(1)III(2)IV(1). Cell 2016;167:1598–609.

[25] Jha P, Wang X, Auwerx J. Analysis of mitochondrial respiratory chain supercomplexes using blue native polyacrylamide gel electrophoresis (BN-PAGE). Curr Protoc Mouse Biol 2016;6:1–14.

[26] Guo R, Zong S, Wu M, Gu J, Yang M. Architecture of human mitochondrial respiratory megacomplex I(2)III(2)IV(2). Cell 2017;170:1247–57.

[27] Acín-Pérez R, Fernández-Silva P, Peleato ML, Pérez-Martos A, Enriquez JA. Respiratory active mitochondrial supercomplexes. Mol Cell 2008;32:529–39.

[28] Rieger B, Shalaeva DN, Söhnel AC, Kohl W, Duwe P, Mulkidjanian AY, et al. Lifetime imaging of GFP at CoxVIIIa reports respiratory supercomplex assembly in live cells. Sci Rep 2017;7:46055.

[29] Paradies G, Paradies V, De Benedictis V, Ruggiero FM, Petrosillo G. Functional role of cardiolipin in mitochondrial bioenergetics. Biochim Biophys Acta – Bioenerg 2014; 1837:408–17.

[30] McKenzie M, Lazarou M, Thorburn DR, Ryan MT. Mitochondrial respiratory chain supercomplexes are destabilized in Barth syndrome patients. J Mol Biol 2006;361: 462–9.

[31] Stroud DA, Surgenor EE, Formosa LE, Reljic B, Frazier AE, Dibley MG, et al. Accessory subunits are integral for assembly and function of human mitochondrial complex I. Nature 2016;538:123–6.

[32] Hirst J, Carroll J, Fearnley IM, Shannon RJ, Walker JE. The nuclear encoded subunits of complex I from bovine heart mitochondria. Biochim Biophys Acta – Bioenerg 2003; 1604:135–50.

[33] Zong S, Wu M, Gu J, Liu T, Guo R, Yang M. Structure of the intact 14-subunit human cytochrome c oxidase. Cell Res 2018;28:1026–34.

[34] Kadenbach B. Regulation of mammalian 13-subunit cytochrome c oxidase and binding of other proteins: role of NDUFA4. Trends Endocrinol Metab 2017;28:761–70.

[35] Hatle KM, Gummadidala P, Navasa N, Bernardo E, Dodge J, Silverstrim B, et al. MCJ/ DnaJC15, an endogenous mitochondrial repressor of the respiratory chain that controls metabolic alterations. Mol Cell Biol 2013;33:2302–14.

[36] Pérez-Pérez R, Lobo-Jarne T, Milenkovic D, Mourier A, Bratic A, García-Bartolomé A, et al. COX7A2L is a mitochondrial complex III binding protein that stabilizes the III₂ +IV supercomplex without affecting respirasome formation. Cell Rep 2016;16: 2387–98.

[37] Lobo-Jarne T, Nývltová E, Pérez-Pérez R, Timón-Gómez A, Molinié T, Choi A, et al. Human COX7A2L regulates complex III biogenesis and promotes supercomplex organization remodeling without affecting mitochondrial bioenergetics. Cell Rep 2018;25:1786–99.

[38] Strogolova V, Furness A, Robb-McGrath M, Garlich J, Stuart RA. Rcf1 and Rcf2, members of the hypoxia-induced gene 1 protein family, are critical components of the mitochondrial cytochrome bc_1-cytochrome c oxidase supercomplex. Mol Cell Biol 2012;32:1363–73.

[39] Vukotic M, Oeljeklaus S, Wiese S, Vögtle FN, Meisinger C, Meyer HE, et al. Rcf1 mediates cytochrome c oxidase assembly and respirasome formation, revealing heterogeneity of the enzyme complex. Cell Metab 2012;15:336–47.

[40] Rathore S, Berndtsson J, Marin-Buera L, Conrad J, Carroni M, Brzezinski P, et al. Cryo-EM structure of the yeast respiratory supercomplex. Nat Struct Mol Biol 2019;26: 50–7.

[41] Chen YC, Taylor EB, Dephoure N, Heo JM, Tonhato A, Papandreou I, et al. Identification of a protein mediating respiratory supercomplex stability. Cell Metab 2012;15: 348–60.

[42] Dienhart MK, Stuart RA. The yeast Aac2 protein exists in physical association with the cytochrome bc_1-COX supercomplex and the TIM23 machinery. Mol Biol Cell 2008;19:3934–43.

[43] Marques I, Dencher NA, Videira A, Krause F. Supramolecular organization of the respiratory chain in Neurospora crassa mitochondria. Eukaryot Cell 2007;6:2391–405.

[44] Jian C, Xu F, Hou T, Sun T, Li J, Cheng H, et al. Deficiency of PHB complex impairs respiratory supercomplex formation and activates mitochondrial flashes. J Cell Sci 2017;130:2620–30.

[45] Vempati UD, Han X, Moraes CT. Lack of cytochrome c in mouse fibroblasts disrupts assembly/stability of respiratory complexes I and IV. J Biol Chem 2009;284:4383–91.

[46] Martínez-Fábregas J, Díaz-Moreno I, González-Arzola K, Díaz-Quintana A, De la Rosa MA. A common signalosome for programmed cell death in humans and plants. Cell Death Dis 2014;5:e1314.

[47] González-Arzola K, Díaz-Moreno I, Cano-González A, Díaz-Quintana A, Velázquez-Campoy A, Moreno-Beltrán B, et al. Structural basis for inhibition of the histone chaperone activity of SET/TAF-Iβ by cytochrome c. Proc Natl Acad Sci U S A 2015; 112:9908–13.

[48] González-Arzola K, Díaz-Quintana A, Rivero-Rodríguez F, Velázquez-Campoy A, De la Rosa MA, Díaz-Moreno I. Histone chaperone activity of Arabidopsis thaliana NRP1 is blocked by cytochrome c. Nucleic Acids Res 2017;45:2150–65.

[49] Osheroff N, Speck SH, Margoliash E, Veerman EC, Wilms J, König BW, et al. The reaction of primate cytochromes c with cytochrome c oxidase. Analysis of the polarographic assay. J Biol Chem 1983;258:5731–8.

[50] Lange C, Hunte C. Crystal structure of the yeast cytochrome bc_1 complex with its bound substrate cytochrome c. Proc Natl Acad Sci U S A 2002;99:2800–5.

[51] Shimada S, Shinzawa-Itoh K, Baba J, Aoe S, Shimada A, Yamashita E, et al. Complex structure of cytochrome c-cytochrome c oxidase reveals a novel protein-protein interaction mode. EMBO J 2017;36:291–300.

[52] Yu CA, Yu L, King TE. Kinetics of electron transfer between cardiac cytochrome c_1 and c. J Biol Chem 1973;248:528–33.

[53] Speck SH, Dye D, Margoliash E. Single catalytic site model for the oxidation of ferrocytochrome c by mitochondrial cytochrome c oxidase. Proc Natl Acad Sci U S A 1984;81:347–51.

[54] Esposti MD, Lenaz G. The kinetic mechanism of ubiquinol: cytochrome c reductase at steady state. Arch Biochem Biophys 1991;289:303–12.

[55] Konermann L, Collings BA, Douglas DJ. Cytochrome c folding kinetics studied by time–resolved electrospray ionization mass spectrometry. Biochemistry 1997;36: 5554–9.

[56] Trouillard M, Meunier B, Rappaport F. Questioning the functional relevance of mitochondrial supercomplexes by time–resolved analysis of the respiratory chain. Proc Natl Acad Sci U S A 2011;108:E1027–34.

[57] Garber EA, Margoliash E. Interaction of cytochrome c with cytochrome c oxidase: an understanding of the high- to low-affinity transition. Biochim Biophys Acta – Bioenerg 1990;1015:279–87.

[58] Speck SH, Margoliash E. Characterization of the interaction of cytochrome c and mitochondrial ubiquinol-cytochrome c reductase. J Biol Chem 1984;259:1064–72.

[59] Moreno-Beltrán B, Díaz-Quintana A, González-Arzola A, Velázquez-Campoy A, De la Rosa MA, Díaz-Moreno I. Cytochrome c_1 exhibits two binding sites for cytochrome c in plants. Biochim Biophys Acta – Bioenerg 2014;1837:1717–29.

[60] Moreno-Beltrán B, Díaz-Moreno I, González-Arzola K, Guerra-Castellano A, Velázquez-Campoy A, De la Rosa MA, et al. Respiratory complexes III and IV can each bind two molecules of cytochrome c at low ionic strength. FEBS Lett 2015; 589:476–83.

[61] Díaz-Moreno I, Díaz-Quintana A, De la Rosa MA, Ubbink M. Structure of the complex between plastocyanin and cytochrome f from the cyanobacterium Nostoc sp. PCC 7119 as determined by paramagnetic NMR. The balance between electrostatic and hydrophobic interactions within the transient complex determines the relative orientation of the two proteins. J Biol Chem 2005;280:18908–15.

[62] Díaz-Moreno I, Hulsker R, Skubak P, Foerster JM, Cavazzini D, Finiguerra MG, et al. The dynamic complex of cytochrome c_6 and cytochrome f studied with paramagnetic NMR spectroscopy. Biochim Biophys Acta 2014;1837:1305–15.

[63] Drepper F, Hippler M, Nitschke W, Haehnel W. Binding dynamics and electron transfer between plastocyanin and photosystem I. Biochemistry 1996;35:1282–95.

[64] Genova ML, Ventura B, Giuliano G, Bovina C, Formiggini G, Parenti Castelli G, et al. The site of production of superoxide radical in mitochondrial complex I is not a bound ubisemiquinone but presumably iron-sulfur cluster N2. FEBS Lett 2001;505: 364–8.

[65] Guerra-Castellano A, Díaz-Quintana A, Pérez-Mejías G, Elena-Real CA, González-Arzola K, García-Mauriño SM, et al. Oxidative stress is tightly regulated by cytochrome c phosphorylation and respirasome factors in mitochondria. Proc Natl Acad Sci U S A 2018;115:7955–60.

[66] Berg OG, von Hippel PH. Diffusion-controlled macromolecular interactions. Annu Rev Biophys Biophys Chem 1985;14:131–60.

[67] Hüttemann M, Lee I, Samavati L, Yu H, Doan JW. Regulation of mitochondrial oxidative phosphorylation through cell signaling. Biochim Biophys Acta 2007;1773: 1701–20.

[68] Hüttemann M, Lee I, Grossman LI, Doan JW, Sanderson TH. Phosphorylation of mammalian cytochrome c and cytochrome c oxidase in the regulation of cell destiny: respiration, apoptosis, and human disease. Adv Exp Med Biol 2012;748: 237–64.

[69] Cruthirds DL, Novak L, Akhi KM, Sanders PW, Thompson JA, MacMillan-Crow LA. Mitochondrial targets of oxidative stress during renal ischemia/reperfusion. Arch Biochem Biophys 2003;412:27–33.

[70] Lee I, Salomon AR, Yu K, Doan JW, Grossma LI, Hüttemann M. New prospects for an old enzyme: mammalian cytochrome *c* is tyrosine-phosphorylated *in vivo*. Biochemistry 2006;45:9121–912.

[71] García-Heredia JM, Díaz-Quintana A, Salzano M, Orzáez M, Pérez-Payá E, Teixeira M, et al. Tyrosine phosphorylation turns alkaline transition into a biologically relevant process and makes human cytochrome *c* behave as an anti-apoptotic switch. J Biol Inorg Chem 2011;16:1155–68.

[72] Zhao X, León IR, Bak S, Mogensen M, Wrzesinski K, Højlund K, et al. Phosphoproteome analysis of functional mitochondria isolated from resting human muscle reveals extensive phosphorylation of inner membrane protein complexes and enzymes. Mol Cell Proteomics 2011;10 [M110.000299].

[73] Sanderson TH, Mahapatra G, Pecina P, Ji Q, Yu K, Sinkler C, et al. Cytochrome *c* is tyrosine 97 phosphorylated by neuroprotective insulin treatment. PLoS One 2013;8: e78627.

[74] García-Heredia JM, Díaz-Moreno I, Díaz-Quintana A, Orzáez M, Navarro JA, Hervás M, et al. Specific nitration of tyrosines 46 and 48 makes cytochrome *c* assemble a non-functional apoptosome. FEBS Lett 2012;586:154–8.

[75] Guerra-Castellano A, Díaz-Moreno I, Velázquez-Campoy A, De la Rosa MA, Díaz-Quintana A. Structural and functional characterization of phosphomimetic mutants of cytochrome *c* at threonine 28 and serine 47. Biochim Biophys Acta – Bioenerg 2016;1857:387–95.

[76] Mahapatra G, Varughese A, Ji Q, Lee I, Liu J, Vaishnav A, et al. Phosphorylation of cytochrome *c* threonine 28 regulates electron transport chain activity in kidney: implications for AMP kinase. J Biol Chem 2017;292:64–79.

[77] Moreno-Beltrán B, Guerra-Castellano A, Díaz-Quintana A, Del Conte R, García-Mauriño SM, Díaz-Moreno S, et al. Structural basis of mitochondrial dysfunction in response to cytochrome *c* phosphorylation at tyrosine 48. Proc Natl Acad Sci U S A 2017;114:E3041–50.

[78] Yu H, Lee I, Salomon AR, Yu K, Hüttemann M. Mammalian liver cytochrome *c* is tyrosine-48 phosphorylated *in vivo*, inhibiting mitochondrial respiration. Biochim Biophys Acta 2008;1777:1066–71.

[79] Kadenbach B. Incorporation of 32P-phosphate into phosphatides of rat liver mitochondria *in vivo* and *in vitro*. FEBS Lett 1968;2:118–20.

[80] Pecina P, Borisenko GG, Belikova NA, Tyurina YY, Pecinova A, Lee I, et al. Phosphomimetic substitution of cytochrome *c* tyrosine 48 decreases respiration and binding to cardiolipin and abolishes ability to trigger downstream caspase activation. Biochemistry 2010;49:6705–14.

[81] Guerra-Castellano A, Díaz-Quintana A, Moreno-Beltrán B, López-Prados J, Nieto PM, Meister W, et al. Mimicking tyrosine phosphorylation in human cytochrome *c* by the evolved tRNA synthetase technique. Eur Chem J 2015;21:15004–12.

[82] Sun J, Trumpower BL. Superoxide anion generation by the cytochrome bc_1 complex. Arch Biochem Biophys 2003;419:198–206.

[83] Genova ML, Lenaz G. The interplay between respiratory Supercomplexes and ROS in aging. Antioxid Redox Signal 2015;23:208–38.

[84] Roberts VA, Pique ME. Definition of the interaction domain for cytochrome *c* on cytochrome *c* oxidase. III. Prediction of the docked complex by a complete, systematic search. J Biol Chem 1999;274:38051–60.

[85] Barrientos A, Pierre D, Lee J, Tzagoloff A. Cytochrome oxidase assembly does not require catalytically active cytochrome *c*. J Biol Chem 2003;278:8881–7.

[86] Welchen E, Hildebrandt TM, Lewejohann D, Gonzalez DH, Braun HP. Lack of cytochrome *c* in *Arabidopsis* decreases stability of complex IV and modifies redox metabolism without affecting complexes I and III. Biochim Biophys Acta – Bioenerg 2012; 1817:990–1001.

[87] Yano N, Muramoto K, Shimada A, Takemura S, Baba J, Fujisawa H, et al. The Mg2+−containing water cluster of mammalian cytochrome *c* oxidase collects four pumping proton equivalents in each catalytic cycle. J Biol Chem 2016;291:23882–94.

[88] Pettersen EF, Goddard TD, Huang CC, Couch GS, Greenblatt DM, Meng EC, et al. UCSF Chimera—a visualization system for exploratory research and analysis. J Comput Chem 2004;25:1605–12.